

# From crystal steps to continuum laws: Behavior near large facets in one dimension

Dionisios Margetis <sup>a,b,c,\*</sup>, Kanna Nakamura <sup>a</sup>

<sup>a</sup>*Department of Mathematics, University of Maryland, College Park, MD 20742*

<sup>b</sup>*Institute for Physical Science and Technology, University of Maryland, College Park, MD 20742*

<sup>c</sup>*Center for Scientific Computation and Mathematical Modeling, University of Maryland, College Park, MD 20742*

---

## Abstract

The passage from discrete schemes for surface line defects (steps) to nonlinear macroscopic laws for crystals is studied via formal asymptotics in one space dimension. Our goal is to illustrate by explicit computations the *emergence* from step equations of continuum-scale power series expansions for the slope near the edges of large, flat surface regions (facets). We consider evaporation-condensation kinetics; and surface diffusion via the Burton, Cabrera and Frank (BCF) model where adsorbed atoms diffuse on terraces and attach-detach at steps. *Nearest-neighbor* step interactions are included. The setting is a monotone train of  $N$  steps separating two semi-infinite facets at fixed heights. We show *how* boundary conditions for the continuum slope and flux, and expansions in the height variable near facets, may emerge from the algebraic structure of discrete schemes as  $N \rightarrow \infty$ . Our technique relies on use of self-similar solutions for discrete slopes; conversion of discrete schemes to sum equations; and their reduction to nonlinear integral equations for the continuum-scale slope. Approximate solutions to the continuum equations near facet edges are constructed by direct iterations. For elastic-dipole step interactions, the continuum slope is found in agreement with a previous hypothesis of “local equilibrium”.

*Key words:* Crystal surface; Epitaxial relaxation; Burton-Cabrera-Frank (BCF) model; Steps; Diffusion; Facets; Macroscopic limit; Nonlinear integral equation

*PACS:* 68.55.-a; 81.10.Aj; 81.15.Aa; 68.35.Md

---

---

\* Corresponding author. Tel.: (301) 405 5455; fax: (301) 314 0827.

*Email addresses:* [dio@math.umd.edu](mailto:dio@math.umd.edu) (Dionisios Margetis),  
[nakamura@math.umd.edu](mailto:nakamura@math.umd.edu) (Kanna Nakamura).

## 1 Introduction

The connection of many-particle schemes to nonlinear partial differential equations (PDEs) has been the subject of extensive studies in non-equilibrium statistical mechanics. This perspective has been explored in various physical contexts; for discussions, see, e.g. [33, 38].

In epitaxial phenomena, “particles” are interacting line defects (steps) of atomic size that move on crystal surfaces by mass conservation [19]. At the nanoscale, the motion of steps is described by large systems of differential equations for step positions. At the macroscale, this description is often reduced conveniently to nonlinear PDEs for macroscopic variables, e.g., for the surface height and slope profiles [7, 15, 20, 24, 28, 30, 34, 41].

The PDEs are believed to be valid away from macroscopically flat surface regions known as “facets”. Spohn [39] treated edges of facets as free boundaries, where in principle boundary conditions for the associated PDEs must be imposed. Such conditions are often formulated within the continuum framework [2, 11, 22, 36, 37, 39, 40] rather than derived directly from steps. The incorporation of facets into continuum evolution laws is a rich, yet largely unexplored, problem [1, 6, 15, 23].

In this paper we address aspects of the question: what are the boundary conditions and near-facet expansions for continuum-scale variables *consistent* with step motion? We focus on two semi-infinite facets separated by a monotone train of  $N$  steps interacting entropically and as elastic dipoles in one space dimension (1D). This setting captures features of a *finite* crystal. From a continuum viewpoint our main results may not be overall surprising: in surface diffusion, the large-scale slope and flux vanish at facet edges. Our technique shows *what local behavior* (in space) of the slope *emerges* from the structure of discrete schemes for crystal steps.

The same system is studied in [11] for *diffusion limited* (DL) kinetics via scaling arguments and numerics for step equations as well as for the PDE describing the slope profile. In this work, a self-similarity *ansatz* is used and verified numerically. However, in [11] the continuum surface slope and flux are *assumed* to vanish at facet edges, with the slope behaving as  $\mathcal{O}(\bar{x}^{1/2})$  for small distances  $\bar{x}$  from the facet edge. These speculations have led to numerical solutions for the continuum slope in excellent agreement with the step simulation data [11].

Here, motivated by the analysis of Al Hajj Shehadeh, Kohn and Weare (AKW) [1], we aim to shed some light on the studies in [11] by adopting a two-scale perspective. First, we use self-similar solutions for finite  $N$  to connect the discrete schemes to a continuum description for the slope as a function of height away from facets. The discrete schemes are converted to sum equations, which

approach integral equations (see Propositions 1-3, Section 3); the latter reveal power series expansions in the height variable. Second, we propose extensions such as *multipole* nearest-neighbor step interactions and special kinetics of extremal steps. We treat evaporation-condensation and surface diffusion in the absence of external material deposition; in fact, the evaporation case is exactly solvable under self-similarity and is invoked for comparisons.

### 1.1 *Microscale: Burton-Cabrera-Frank (BCF) model*

It is of interest to review elements of epitaxy for crystals; for extensive reviews, see, e.g., [9, 14, 26, 31, 32]. The morphological evolution of crystal surfaces is driven by the motion of atomic steps separating nanoscale terraces, as was first predicted by Burton, Cabrera and Frank (“BCF”) [4]. Three basic ingredients of the BCF model for surface diffusion are: (i) motion of steps by mass conservation; (ii) diffusion of adsorbed atoms (“adatoms”) on terraces; and (iii) attachment and detachment of atoms at steps.

Another transport process included here is evaporation-condensation: atoms are exchanged between step edges and the surrounding vapor. We neglect atom desorption on terraces and diffusion along step edges [19]; and leave out material deposition from above. Hence, the surface is expected to relax by lowering its energy. Furthermore, we consider entropic and elastic-dipole *nearest-neighbor* step interactions [19, 21, 27]; see Section 4.1 for an extension.

### 1.2 *Macroscopic limit and previous works*

The BCF framework is our starting point. In the macroscopic limit the step size approaches zero while the step density is kept fixed. Our analysis is formal, i.e., it invokes simplifying assumptions (which may be provable) and avoids rigor. For instance, starting with a monotone step train (at  $t = 0$ ), we assume that the discrete slopes,  $m_j(t)$  ( $j$ : step number,  $t$ : time), and continuum-scale slope,  $m(h, t)$  ( $h$ : height), are positive on the sloping surface for  $t > 0$  and the continuum limit makes sense. We posit self-similarity for finite  $N$ ; presumably, this is reached for long enough times [1, 11] in various kinetic regimes, but this property is not proved here. The persistence of semi-infinite facets during evolution is hypothesized.

This formal approach enables us to explore modifications of the energetics and kinetics of the step model. Our arguments indicate how microscale mechanisms can control the slope behavior at the macroscale.

Our work has been inspired by AKW [1]. These authors study rigorously

the relaxation of the same step configuration by employing the  $l^2$ -steepest descent of a discrete energy functional under *attachment-detachment limited* (ADL) kinetics. In this case, the dominant process is the exchange of atoms at step edges. Notably, AKW invoke ordinary differential equations (ODEs) for *discrete slopes* at the nanoscale, and a PDE for the surface slope as a function of height at the macroscale. In [1], the positivity of discrete slopes and convergence of the discrete self-similar solution to a continuum self-similar one with zero slope at facet edges are proved; the condition of zero flux emerges as a “natural boundary condition” from the steepest descent. An analogous method for DL kinetics appears elusive at the moment.

Israeli, Jeong, Kandel and Weeks [17] study self-similar slope profiles under evaporation-condensation and surface diffusion with ADL kinetics for three 1D step geometries. Their step trains are semi-infinite and thus differ from the *finite* step train studied here and in [1]. For this reason, direct comparisons to results of [17] are not compelling. By contrast to our setting, the self-similar slopes in [1] do not decay with time. In the same work [17], the condition of zero slope at the facet edge along with a power series expansion of a certain form for the slope are imposed at the outset. Because of the different boundaries involved, their scaling exponent (in the self-similarity variable) and form of the power series for evaporation-condensation are different from ours.

We adopt the use of the height as an independent variable [1], which is a convenient Lagrangian coordinate of motion [10, 11]. An advantage of this choice in the present setting, where facets are at fixed heights, is the elimination of free boundaries, as pointed out by AKW. We invoke equations for the discrete slopes, following AKW as well as Israeli and Kandel [15, 16].

### 1.3 Goals and paper organization

Our intention with the present work is twofold. First, we aim to illustrate explicitly how boundary conditions for the continuum-scale slope and flux, and power series expansions in the space coordinate for the slope, are plausibly related to the algebraic structure of the discrete laws. In surface diffusion, this structure consists of three difference schemes: (i) the step velocity in terms of flux; (ii) the flux in terms of step chemical potential (a thermodynamic force); and (iii) the step chemical potential in terms of the discrete slope cubed for elastic-dipole step interactions. Our method addresses DL and ADL kinetics.

Our second goal is to test the hypothesis of “local equilibrium”, often applied for facet edges within continuum [11, 22]. By this hypothesis, the surface slope vanishes as the square root of the distance from edges of zero-slope facets, if steps interact as elastic dipoles. This behavior is speculated by analogy

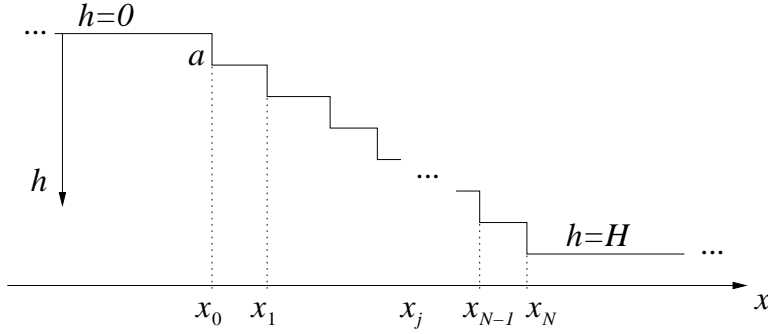


Fig. 1. Geometry in 1D (cross section): the step height is  $a$ ; the step position is  $x_j$ ; and the semi-infinite facets are located at heights  $h = 0$  (top) and  $h = H$  (bottom).

with equilibrium crystal shapes on the basis of a surface free energy density proportional to the slope cubed [3, 13, 18]. A different local behavior is pointed out in [17] for evaporation-condensation kinetics.

The remainder of the paper is organized as follows. In Section 2, we formulate ODEs for discrete slopes. In Section 3, we study the emergence from discrete schemes of continuum-scale expansions for the slope near facets. In Section 4, we discuss possible extensions. Section 5 summarizes our results.

*Units.* We use nondimensional quantities via scaling of coordinates and other variables. The atomic area, terrace diffusivity, Boltzmann energy ( $k_B T$ ) and step-step interaction strength are set equal to unity, since the respective dimensional parameters can be consolidated into a time scale.

## 2 Formulation: Step motion laws

The step geometry is shown in Fig. 1. The system consists of  $N + 1$  steps at positions  $x = x_j(t)$  where  $j = 0, \dots, N$  and  $t \geq 0$ . The steps have constant size  $a$ , and separate two semi-infinite plateaus at fixed heights,  $h = 0$  for  $x < x_0(t)$  and  $h = H \gg a$  for  $x > x_N(t)$ ; cf. [1, 11].

Set  $\tilde{x} = x/H$  and  $\tilde{h} = h/H$  and drop the tildes; thus,  $(N + 1)\epsilon = 1$  (where  $N \gg 1$  and  $\epsilon \ll 1$ ),  $0 \leq h \leq 1$  and  $a$  is replaced by  $\epsilon = a/H$ . Following AKW, we employ  $m_j$  as dependent variables. Further, we *assume* that the discrete step slopes,  $m_j$ , are positive for all  $t > 0$ , given that  $m_j > 0$  at  $t = 0$ :

$$m_j(t) := \frac{\epsilon}{x_{j+1}(t) - x_j(t)} > 0, \quad j = 0, 1, \dots, N - 1. \quad (1)$$

Next, we describe thermodynamic elements of step motion, which permeate both evaporation-condensation and surface diffusion processes. For entropic

and elastic-dipole step interactions, the energy of the step train is [19, 21, 27]

$$E_N = \frac{1}{2} \sum_{i=0}^{N-1} \left( \frac{\epsilon}{x_{i+1} - x_i} \right)^2 = \frac{1}{2} \sum_{i=0}^{N-1} m_i^2 . \quad (2)$$

The chemical potential of the  $j$ th step is [19]

$$\mu_j = \frac{\delta E_N}{\delta x_j} = \epsilon^{-1} \left[ \left( \frac{\epsilon}{x_{j+1} - x_j} \right)^3 - \left( \frac{\epsilon}{x_j - x_{j-1}} \right)^3 \right] = \epsilon^{-1} (m_j^3 - m_{j-1}^3) \quad (3a)$$

if  $j = 1, \dots, N-1$ ; for the *extremal* steps at  $x = x_0, x_N$  we have

$$\mu_0 = \epsilon^{-1} m_0^3 , \quad \mu_N = -\epsilon^{-1} m_{N-1}^3 . \quad (3b)$$

In order to prescribe the step velocity law, we first have to specify the dominant mass transport mechanism. In evaporation-condensation, the step velocity,  $v_j$ , is driven by the step chemical potential [19, 39]. By contrast, in surface diffusion,  $v_j$  is driven by differences of adatom fluxes across step edges.

### 2.1 Evaporation-condensation process

For a specific version of this process, the step velocity law reads [19, 39, 40]

$$v_j(t) = \frac{dx_j(t)}{dt} = \dot{x}_j(t) = -(\mu_j - \mu^0) \quad (j = 0, 1, \dots, N) , \quad (4)$$

where  $\mu^0$  is the chemical potential of the surrounding vapor; set  $\mu^0 = 0$  since only  $v_{j+1} - v_j$  will matter. In (4), we use a constant mobility; see [32, 39, 40] for variants of (4). In view of (3), we wind up with the discrete scheme

$$\dot{m}_0 = -\epsilon^{-1} m_0^2 (\dot{x}_1 - \dot{x}_0) = \epsilon^{-2} m_0^2 (m_1^3 - 2m_0^3) , \quad (5a)$$

$$\dot{m}_j = \epsilon^{-2} m_j^2 (m_{j+1}^3 - 2m_j^3 + m_{j-1}^3) , \quad j = 1, \dots, N-2 , \quad (5b)$$

$$\dot{m}_{N-1} = \epsilon^{-2} m_{N-1}^2 (m_{N-2}^3 - 2m_{N-1}^3) . \quad (5c)$$

Equations (5) are consolidated into the law

$$\epsilon^{-2} m_j^2 (m_{j+1}^3 - 2m_j^3 + m_{j-1}^3) = \dot{m}_j , \quad j = 0, \dots, N-1 , \quad (6a)$$

along with the termination conditions

$$m_{-1} = 0 = m_N . \quad (6b)$$

Heuristically, we can eliminate time via the (particular) self-similar solution

$$m_j(t) = P(t) M_j \quad (dM_j/dt \equiv 0, M_j \neq 0). \quad (7)$$

This choice is compatible with the structure of discrete equations (6). By (6), we have  $\dot{p}/p^5 = -C = \text{const.}$  and set  $C = 1$  for later algebraic convenience; thus,  $P(t) = (4t + K)^{-1/4}$ . So,  $M_j$  satisfy the *second-order* difference scheme

$$M_{j+1}^3 - 2M_j^3 + M_{j-1}^3 = -\frac{\epsilon^2}{M_j}, \quad j = 0, \dots, N-1 \quad (M_j > 0), \quad (8a)$$

$$M_{-1} = 0 = M_N. \quad (8b)$$

In Section 3.1, we show *how* the discrete termination conditions (8b) give rise to a vanishing continuum-scale slope as  $j \rightarrow \infty$  with  $h = (j+1)\epsilon = \mathcal{O}(1) \ll 1$ . The (local) behavior of the slope near facets is manifested accordingly.

## 2.2 Surface diffusion process

The step velocity law is

$$v_j = \dot{x}_j = \epsilon^{-1}[\varphi_{j-1}(x_j) - \varphi_j(x_j)], \quad j = 1, \dots, N-1; \quad (9)$$

$\varphi_j(x) = -\partial_x \rho_j(x)$  is the adatom flux on the  $j$ th terrace,  $\{x_j < x < x_{j+1}\}$  (where the diffusivity is set to unity). The adatom density  $\rho_j(x)$  satisfies  $\partial_x^2 \rho_j = \partial_t \rho_j \approx 0$  in the quasisteady regime [19], where steps move slower than adatoms diffuse. We have  $\rho_j(x) = A_j x + B_j$  in  $\{x_j < x < x_{j+1}\}$ ,  $j = 0, \dots, N-1$ , and the atom attachment-detachment conditions

$$-\varphi_j = 2\kappa(\rho_j - \rho_j^{\text{eq}})\Big|_{x_j}, \quad \varphi_j = 2\kappa(\rho_j - \rho_{j+1}^{\text{eq}})\Big|_{x_{j+1}}, \quad (10)$$

where  $2\kappa$  is a kinetic rate for the exchange of atoms at a step edge, the factor of 2 is included for later algebraic convenience, and  $\rho_j^{\text{eq}} = 1 + \mu_j$  is an equilibrium density (by  $k_B T = 1$ ) [19]. By enforcement of (10), we compute  $A_j$ :

$$\varphi_j(x) = -A_j = -\frac{\kappa}{1 + \kappa(x_{j+1} - x_j)}(\mu_{j+1} - \mu_j), \quad j = 0, \dots, N-1. \quad (11a)$$

Equation (9) needs to be extended to  $j = 0, N$ . By taking into account  $\rho_j(x)$  for  $j = -1, x < x_0$  and  $j = N, x > x_N$ , where there are no steps and  $\rho_j(x)$  must be bounded in  $x$ , we find the plateau fluxes

$$\varphi_{-1}(x) = 0 \quad x < x_0, \quad \varphi_N(x) = 0 \quad x > x_N. \quad (11b)$$

Next, we combine (9) and (11) with (3) to obtain a system of ODEs for  $m_j$ :

$$\frac{\dot{m}_0}{m_0^2} = -\epsilon^{-4} \left[ \frac{\kappa\epsilon}{m_1 + \kappa\epsilon} m_1 (m_2^3 - 2m_1^3 + m_0^3) - \frac{2\kappa\epsilon}{m_0 + \kappa\epsilon} m_0 (m_1^3 - 2m_0^3) \right], \quad (12a)$$

$$\begin{aligned} \frac{\dot{m}_1}{m_1^2} = & -\epsilon^{-4} \left[ \frac{\kappa\epsilon}{m_2 + \kappa\epsilon} m_2 (m_3^3 - 2m_2^3 + m_1^3) - \frac{2\kappa\epsilon}{m_1 + \kappa\epsilon} \right. \\ & \left. \times m_1 (m_2^3 - 2m_1^3 + m_0^3) + \frac{\kappa\epsilon}{m_0 + \kappa\epsilon} m_0 (m_1^3 - 2m_0^3) \right], \end{aligned} \quad (12b)$$

$$\begin{aligned} \frac{\dot{m}_j}{m_j^2} = & -\epsilon^{-4} \left[ \frac{\kappa\epsilon}{m_{j+1} + \kappa\epsilon} m_{j+1} (m_{j+2}^3 - 2m_{j+1}^3 + m_j^3) - \frac{2\kappa\epsilon}{m_j + \kappa\epsilon} m_j (m_{j+1}^3 \right. \\ & \left. - 2m_j^3 + m_{j-1}^3) + \frac{\kappa\epsilon}{m_{j-1} + \kappa\epsilon} m_{j-1} (m_j^3 - 2m_{j-1}^3 + m_{j-2}^3) \right], \\ & j = 2, \dots, N-3, \end{aligned} \quad (12c)$$

$$\begin{aligned} \frac{\dot{m}_{N-2}}{m_{N-2}^2} = & -\epsilon^{-4} \left[ \frac{\kappa\epsilon}{m_{N-3} + \kappa\epsilon} m_{N-3} (m_{N-4}^3 - 2m_{N-3}^3 + m_{N-2}^3) \right. \\ & - \frac{2\kappa\epsilon}{m_{N-2} + \kappa\epsilon} m_{N-2} (m_{N-3}^3 - 2m_{N-2}^3 + m_{N-1}^3) \\ & \left. + \frac{\kappa\epsilon}{m_{N-1} + \kappa\epsilon} m_{N-1} (m_{N-2}^3 - 2m_{N-1}^3) \right], \end{aligned} \quad (12d)$$

$$\begin{aligned} \frac{\dot{m}_{N-1}}{m_{N-1}^2} = & -\epsilon^{-4} \left[ \frac{\kappa\epsilon}{m_{N-2} + \kappa\epsilon} m_{N-2} (m_{N-3}^3 - 2m_{N-2}^3 + m_{N-1}^3) \right. \\ & \left. - \frac{2\kappa\epsilon}{m_{N-1} + \kappa\epsilon} m_{N-1} (m_{N-2}^3 - 2m_{N-1}^3) \right]. \end{aligned} \quad (12e)$$

Equations (12) are simplified in two regimes: (i) ADL kinetics [1], where  $m_j \gg \kappa\epsilon$  for all  $j$ ; and (ii) DL kinetics [11], where  $\kappa\epsilon \gg m_j$ .

*ADL kinetics.* Equations (12) are reduced to the ODEs

$$\frac{\dot{m}_j}{m_j^2} = -\epsilon^{-4}(m_{j+2}^3 - 4m_{j+1}^3 + 6m_j^3 - 4m_{j-1}^3 + m_{j-2}^3), \quad (13a)$$

for  $j = 0, \dots, N-1$ , along with the conditions

$$m_{-1} = 0 = m_N, \quad m_0^3 - 2m_{-1}^3 + m_{-2}^3 = 0 = m_{N-1}^3 - 2m_N^3 + m_{N+1}^3. \quad (13b)$$

In (13a), we have set  $\kappa\epsilon = 1$  by appropriately rescaling time.

In particular, by the ansatz  $m_j(t) = P(t)M_j$ , we find  $P(t) = (Ct + K)^{-1/4}$  and set  $C = 4$ , assuming  $M_j > 0$ . This solution is approached for long enough times [1]. Consequently,  $M_j$  satisfies the *fourth-order* difference scheme

$$M_{j+2}^3 - 4M_{j+1}^3 + 6M_j^3 - 4M_{j-1}^3 + M_{j-2}^3 = \frac{\epsilon^4}{M_j}, \quad j = 0, \dots, N-1, \quad (14a)$$

$$M_{-1} = 0 = M_N, \quad M_0^3 - 2M_{-1}^3 + M_{-2}^3 = 0 = M_{N-1}^3 - 2M_N^3 + M_{N+1}^3. \quad (14b)$$

*DL kinetics.* With recourse to (12) we obtain the ODEs

$$\begin{aligned} \frac{\dot{m}_j}{m_j^2} = & -\epsilon^{-4}[m_{j+1}(m_{j+2}^3 - 2m_{j+1}^3 + m_j^3) - 2m_j(m_{j+1}^3 - 2m_j^3 + m_{j-1}^3) \\ & + m_{j-1}(m_j^3 - 2m_{j-1}^3 + m_{j-2}^3)], \quad j = 0, \dots, N-1, \end{aligned} \quad (15a)$$

where

$$m_{-1} = 0 = m_N, \quad m_{-2}, m_{N+1} : \text{finite}; \quad (15b)$$

so,  $m_{-1}(m_0^3 - 2m_{-1}^3 + m_{-2}^3) = 0 = m_N(m_{N-1}^3 - 2m_N^3 + m_{N+1}^3)$ .

Now suppose  $m_j(t) = P(t)M_j$ . By (15) we have  $\dot{p}/p^6 = -C < 0$  and find  $P(t) = (5Ct + K)^{-1/5}$ ; set  $C = 1$ . The ensuing difference equation for  $M_j$  is

$$\begin{aligned} M_{j+1}(M_{j+2}^3 - 2M_{j+1}^3 + M_j^3) - 2M_j(M_{j+1}^3 - 2M_j^3 + M_{j-1}^3) \\ + M_{j-1}(M_j^3 - 2M_{j-1}^3 + M_{j-2}^3) = \frac{\epsilon^4}{M_j}, \quad j = 0, \dots, N-1, \end{aligned} \quad (16a)$$

with  $M_j > 0$  for  $j \in \{0, 1, \dots, N-1\}$  and conditions

$$M_{-1} = 0 = M_N \quad \text{and} \quad M_{-2}, M_{N+1} : \text{finite}. \quad (16b)$$

It is tempting to presume that conditions (13b), (15b) imply automatically a zero continuum-scale slope and flux at the facet edge. The study of *how* discrete conditions (16b) induce asymptotically respective power series expansions to continuum solutions near facets is the subject of Section 3.2.

### 3 Limit of discrete scheme and near-facet expansions

In this section we derive expansions for the continuum-scale slope near facet edges *directly* from discrete schemes for steps. The idea is to convert the discrete schemes to sum equations; and show that, in the limit  $\epsilon \downarrow 0$  with  $h = (j + 1)\epsilon = \mathcal{O}(1)$  and  $(N + 1)\epsilon = 1$ , the sum equations become integral equations which indicate via iterations the slope behavior as  $h \downarrow 0$  and  $h \uparrow 1$ .

In the limit  $\epsilon \downarrow 0$ , we assume that the discrete slopes,  $m_j$ , approach the surface slope in an appropriate weak sense [25]. In principle, given a sequence  $\{u_j\}_{j=0}^{N-1}$  (e.g.,  $u = m$ ), we posit a continuous  $u(h, t)$ ,  $h \in (0, 1)$ , such that for every (smooth) test function  $\vartheta(h)$  with  $\vartheta_j := \vartheta((j + 1)\epsilon)$  and  $t > 0$  we have

$$\epsilon \sum_{j=0}^{N-1} \vartheta_j u_j(t) = (N + 1)^{-1} \sum_{j=0}^{N-1} \vartheta_j u_j(t) \xrightarrow{N \rightarrow \infty} \int_0^1 \vartheta(h) u(h, t) dh . \quad (17)$$

We write  $u_j(\cdot) \rightharpoonup u(h, \cdot)$  to imply the weak limit (17). Further, we assume convergence of the related sums and integrals in order to simplify derivations, thus relaxing rigor.

Regarding the behavior of  $m(h, t)$  near facets, the *order of limits* should be emphasized. *First*, we let  $\epsilon \downarrow 0$  with fixed  $h$ ; *next*, we allow  $h \downarrow 0$  or  $h \uparrow 1$ .

#### 3.1 Evaporation-condensation kinetics

Consider slopes under self-similarity,  $m_j(t) = (4Ct + K)^{-1/4} M_j$ , and set  $C = 1$ ; more generally, a constant  $C \neq 1$  would enter the resulting integral equation for  $m(h)$  as a prefactor of the integral term. The analysis is not essentially different if we consider  $C \neq 1$ . Start with (8). This case helps validate our approach; the reasons become more clear below. By  $\psi_j := M_j^3$ , the relevant difference scheme reads

$$\psi_{j+1} - 2\psi_j + \psi_{j-1} = f_j = -\frac{\epsilon^2}{\psi_j^{1/3}}, \quad \psi_{-1} = 0 = \psi_N , \quad (18)$$

where  $\psi_j > 0$  and  $j = 0, 1, \dots, N - 1$ .

**Proposition 1.** (A continuum limit in evaporation-condensation) *In the limit  $\epsilon \downarrow 0$ , discrete scheme (18) reduces to the integral equation*

$$\psi(h) = m(h)^3 = C_1 h - \int_0^h \frac{h - z}{m(z)} dz \quad 0 < h < 1 ; \quad (19)$$

thus,  $\lim_{h \downarrow 0} m(h) = 0$ . The constant  $C_1$  is

$$C_1 = \int_0^1 \frac{1-z}{\psi(z)^{1/3}} dz = \int_0^1 \frac{1-z}{m(z)} dz, \quad (20)$$

which implies  $\lim_{h \uparrow 1} m(h) = 0$ . By (19), a sufficiently differentiable  $m(h)$  satisfies the ODE  $m(m^3)_{hh} = -1$  for  $0 < h < 1$ .

By abusing notation, we use the symbol  $m(h)$  for the space-dependent part of the self-similar slope; i.e.,  $m(h, t) = P(t)m(h)$ . Assume that the integral in (19) converges and a solution exists in an appropriate sense.

**Proof.** By (18), we express  $\psi_j$  in terms of a finite sum over  $f_j$ , exploiting the structure of the difference equations. To this aim, we write

$$\psi_j = \left. \frac{1}{j!} \frac{d^j \Psi(s)}{ds^j} \right|_{s=0} = \frac{1}{2\pi i} \oint_{\Gamma} \frac{\Psi(\zeta)}{\zeta^{j+1}} d\zeta \quad (i^2 = -1), \quad j = 0, \dots, N-1, \quad (21)$$

by applying the Cauchy integral formula, where  $\Gamma$  is a contour enclosing 0 and  $\Psi(s)$  is the generating function (polynomial) defined by

$$\Psi(s) = \sum_{j=0}^{N-1} \psi_j s^j \quad s \in \mathbb{C}. \quad (22)$$

This  $\Psi(s)$  is computed via (18); see Appendix A.1 for details. The result is

$$\Psi(s) = \frac{\psi_0 + \psi_{N-1} s^{N+1} + sF(s)}{(1-s)^2}, \quad F(s) = \sum_{j=0}^{N-1} f_j s^j, \quad (23)$$

where  $\psi_0, \psi_{N-1}$  are such that  $s = 1$  is a removable singularity of  $\Psi(s)$ :

$$\psi_0 = \frac{-NF(1) + F'(1)}{N+1}, \quad \psi_{N-1} = -\frac{F(1) + F'(1)}{N+1}. \quad (24)$$

The prime denotes the derivative of  $F(s)$ . By (21), we find (see Appendix A.1)

$$\psi_j = (1+j)\psi_0 + \sum_{p=0}^{j-1} (j-p)f_p = (1+j)\psi_0 - \sum_{p=0}^{j-1} \epsilon [(j+1)\epsilon - (p+1)\epsilon] \psi_p^{-1/3}. \quad (25)$$

This is the desired sum equation for  $\psi_j$ .

Let us now focus on the limit of (25) as  $\epsilon \downarrow 0$  with  $(j+1)\epsilon = h = \mathcal{O}(1)$ . With regard to the computation of  $\psi_0$  by (24), note that

$$(N+1)\psi_0 = \sum_{j=0}^{N-1} [(N+1)\epsilon - (j+1)\epsilon] \psi_j^{-1/3} \epsilon \xrightarrow{\epsilon \downarrow 0} \int_0^1 (1-h)\psi(h)^{-1/3} dh, \quad (26)$$

assuming that the respective sum and integral are convergent; thus,

$$\lim_{\epsilon \downarrow 0} (\epsilon^{-1} \psi_0) =: C_1 = \int_0^1 \frac{1-h}{\psi(h)^{1/3}} dh = \int_0^1 \frac{1-h}{m(h)} dh. \quad (27)$$

Let  $z = (p+1)\epsilon$  in (25); then, by  $\psi_p \rightarrow \psi(z)$ , we have

$$\sum_{p=0}^{j-1} [(j+1)\epsilon - (p+1)\epsilon] \psi_p^{-1/3} \epsilon \rightarrow \int_0^h (h-z) \psi(z)^{-1/3} dz. \quad (28)$$

This limit is encapsulated in the Euler summation formula; see, e.g., [5]. In view of (27), we wind up with (19) and (20). The ODE  $m(m^3)_{hh} = -1$  ensues by differentiation (in the usual calculus sense) of the integral equation. This assertion concludes our formal derivation.  $\square$

**Corollary 1.** *The constant  $C_1$  appearing in (19) is positive.*

*Near-facet expansion.* Proposition 1 suggests what the behavior of  $m$  near facet edges should be. Notice that the integral in (19) produces a subdominant contribution  $\mathcal{O}(h^{2-\alpha})$  if  $m(h) = \mathcal{O}(h^\alpha)$  as  $h \downarrow 0$  for some  $0 \leq \alpha < 1$ . A formal expansion can be derived by *iteration* of (19). (We alert the reader that our construction of a local self-similar solution by iteration is heuristic. A rigorous analysis lies beyond our present scope.) Set  $m(h) \sim m^{(n)}(h)$  to  $n+1$  terms as  $h \downarrow 0$ , where

$$m^{(n+1)}(h)^3 = C_1 h - \int_0^h \frac{h-z}{m^{(n)}(z)} dz; \quad m^{(0)}(h) = (C_1 h)^{1/3}, \quad (29)$$

and  $n = 0, 1, \dots$ . Thus, we derive the three-term expansion

$$m(h) = (C_1 h)^{1/3} - \frac{3}{10} C_1^{-1} h - \frac{171}{1400} C_1^{-7/3} h^{5/3} + \mathcal{O}(h^{7/3}) \quad \text{as } h \downarrow 0; \quad (30)$$

higher-order terms are produced directly. Our construction satisfies the estimate  $m^{(n+1)} - m^{(n)} = \mathcal{O}(h^{2n/3+1})$ . Expansion (30) is in agreement with the corresponding exact, global solution; see discussion in Appendix B.1.

The formal expansion by iteration can be converted to a power series in  $x - x_{f,L}$  where  $x_{f,L}(t)$  is the position of the left facet edge. By  $\dot{x}_j = -\mu_j = -\epsilon^{-1}(m_j^3 - m_{j-1}^3)$ , and the ansatz  $m_j(t) = (4t + K)^{-1/4} M_j$ , we ascertain that  $x_j(t) \sim t^{1/4} X_j$  for large  $t$ . Hence, the similarity coordinate is  $\eta = xt^{-1/4}$  and we set  $h = h(\eta)$ ;  $m(h(\eta)) = h'(\eta)$ . By integrating (30), after some algebra we obtain

$$C_1^{1/3} (\eta - \eta_{f,L}) = \frac{3}{2} h^{2/3} + \frac{9}{40} C_1^{-4/3} h^{4/3} + \frac{1305}{2800} C_1^{-8/3} h^2 + \mathcal{O}(h^{8/3}) \quad \text{as } h \downarrow 0,$$

where  $\eta_{f,L} = x_{f,L}(t)t^{-1/4}$ . By inverting in the limit  $\bar{\eta} = \eta - \eta_{f,L} \downarrow 0$ , we find

$$m(h(\eta)) = \left(\frac{2}{3}\right)^{3/2} C_1^{1/2} \left[ \frac{3}{2} \bar{\eta}^{1/2} - \frac{3}{8} C_1^{-1} \bar{\eta}^{3/2} - \frac{971}{1600} C_1^{-2} \bar{\eta}^{5/2} + \mathcal{O}(\bar{\eta}^{7/2}) \right]. \quad (31)$$

For the other end point ( $h \uparrow 1$ ), mirror symmetry applies (under  $h \mapsto 1 - h$ ).

**Remark 1.** Integral equation (19) can result from integrating the ODE  $(m^3)_{hh} = -1/m$  via imposing from the outset  $m \rightarrow 0$  as  $h \downarrow 0$  and  $h \uparrow 1$ . Here, we let this zero-slope condition emerge by directly resolving the discrete scheme.

**Remark 2.** It is tempting to extend the above calculation to the full time-dependent setting, with focus on ODEs (6). Consider  $m_j(t) \mapsto m(h, t)$ . Formally,  $1/m(h)$  (under self-similarity) is now replaced by  $\partial_t[m(h, t)^{-1}]$  in defining  $f_j$ . If the integral converges, the relation for  $m(h, t)$  now reads

$$m(h, t)^3 = C_1(t)h - \int_0^h (h - z) \partial_t[m(z, t)^{-1}] dz \quad t > 0; \quad (32)$$

$C_1(t)$  is given by the  $t$ -dependent counterpart of (20). Alternatively, differentiate to get the PDE  $\partial_t m = m^2 \partial_h^2 (m^3)$  [40]. Caution should be exercised though: in principle, (32) may not be amenable to iterations in the sense described above, unless  $t$  is sufficiently large. So, it is not advisable to iterate (32) to study transients of the slope near the facet edge.

**Remark 3.** This discussion suggests that, for a class of initial data,

$$m(h(x, t), t) = \mathcal{O}((x - x_f(t))^{1/2}) \quad x \rightarrow x_f(t), \quad (33)$$

at the left- and right-facet edge position,  $x_f(t)$ , for sufficiently long times. Notably, this behavior is in agreement with the condition of local equilibrium at facet edges [3,18]. Furthermore, the integral equation formulation indicates the *form* of the expansion for  $m(h, t)$  and readily provides the leading-order term. For the derivation of higher-order terms (to arbitrary order), it is algebraically convenient to use the respective PDE (or ODE for self-similar slopes). The starting point is the power series expansion  $\sum_{n=1}^{\infty} A_n (x - x_f(t))^{n/2}$ , in accord with the iterations of (19); see also Section 3.2. This form is to be contrasted with the series used in [17] for a geometry having a single semi-infinite facet, where the self-similar solution for the continuum slope does not decay in time.

### 3.2 Surface diffusion

Our analysis for evaporation-condensation can be extended to surface diffusion with a few (mostly technical) modifications. For DL kinetics, we split the fourth-order discrete scheme into two second-order schemes. This case is

discussed in some detail. We present fewer details for ADL kinetics where the fourth-order scheme is treated without analogous splitting.

### 3.2.1 DL kinetics

We first focus on the self-similarity ansatz  $m_j(t) = (5t + K)^{-1/5} M_j$  observed in [11], and set  $\psi_j = M_j^3$ . The fourth-order scheme (16) is split as

$$\psi_{j+1} - 2\psi_j + \psi_{j-1} = -\frac{\epsilon^2 \varphi_j}{\psi_j^{1/3}}, \quad \varphi_{j+1} - 2\varphi_j + \varphi_{j-1} = -\frac{\epsilon^2}{\psi_j^{1/3}}; \quad (34a)$$

$$\psi_{-1} = 0 = \psi_N, \quad \varphi_{-1} = 0 = \varphi_N; \quad j = 0, 1, \dots, N-1. \quad (34b)$$

Recall that  $\varphi_j$  is the adatom flux on the  $j$ th terrace, where  $x_j < x < x_{j+1}$ .

**Proposition 2.** (A continuum limit in DL kinetics) *In the limit  $\epsilon \downarrow 0$ , discrete scheme (34) reduces to the integral equation*

$$\psi(h) = m(h)^3 = C_1 h - C_2 \int_0^h \frac{z(h-z)}{m(z)} dz + \int_0^h \int_0^z \frac{(h-z)(z-\zeta)}{m(z)m(\zeta)} d\zeta dz, \quad (35)$$

for  $0 < h < 1$ ; thus,  $\lim_{h \downarrow 0} m(h) = 0 = \lim_{h \downarrow 0} \varphi(h)$  ( $\varphi$ : flux). The constants  $C_1, C_2$  are subject to respective conditions at  $h = 1$ :  $\lim_{h \uparrow 1} m(h) = 0 = \lim_{h \uparrow 1} \varphi(h)$ . By (35), any sufficiently differentiable  $m(h)$  satisfies  $m[m(m^3)_{hh}]_{hh} = 1$ .

In fact, (34) reduces to a pair of integral relations, which yield (35). The primary continuum variables are the slope,  $m(h)$ , and flux,  $\varphi(h)$ ; see (38),(39). Assume that the integrals in (35) converge and a solution exists appropriately.

**Proof.** We proceed along the lines of Section 3.1; recall formulas (21) and (22) regarding  $\psi_j$  in terms of  $\Psi(s)$ . Our strategy is to express each of the second-order difference equations (34a) as a sum equation, treating their right-hand sides as forcing terms,  $f_j$  (see Appendix A.1). The first one of (34a) leads to

$$\psi_j = (1+j)\psi_0 - \sum_{p=0}^{j-1} [(j+1)\epsilon - (p+1)\epsilon] \frac{\varphi_p}{\psi_p^{1/3}} \epsilon, \quad (36a)$$

after applying the first pair of conditions (34b); the coefficient  $\psi_0$  is given by

$$(N+1)\psi_0 = \sum_{j=0}^{N-1} [(N+1)\epsilon - (j+1)\epsilon] \frac{\varphi_j}{\psi_j^{1/3}} \epsilon. \quad (36b)$$

The second one of equations (34a) with the last pair of conditions (34b) yield

$$\varphi_j = (1+j)\varphi_0 - \sum_{p=0}^{j-1} \frac{(j+1)\epsilon - (p+1)\epsilon}{\psi_p^{1/3}} \epsilon, \quad (37a)$$

where, by analogy with (36b),

$$(N+1)\varphi_0 = \sum_{j=0}^{N-1} [(N+1)\epsilon - (j+1)\epsilon] \psi_j^{-1/3} \epsilon. \quad (37b)$$

Now let  $\epsilon \downarrow 0$  with  $(N+1)\epsilon = 1$  and  $(j+1)\epsilon = h = \mathcal{O}(1)$ . By (36), we have

$$\psi_j \rightarrow \psi(h) = m(h)^3 = C_1 h - \int_0^h (h-z) \frac{\varphi(z)}{m(z)} dz \quad 0 < h < 1; \quad (38a)$$

$$C_1 := \lim_{\epsilon \downarrow 0} (\epsilon^{-1} \psi_0) = \int_0^1 (1-z) \frac{\varphi(z)}{m(z)} dz. \quad (38b)$$

By (37), the analogous limit for  $\varphi_j$  is

$$\varphi_j \rightarrow \varphi(h) = C_2 h - \int_0^h \frac{h-z}{m(z)} dz \quad 0 < h < 1; \quad (39a)$$

$$C_2 := \lim_{\epsilon \downarrow 0} (\epsilon^{-1} \varphi_0) = \int_0^1 \frac{1-z}{m(z)} dz. \quad (39b)$$

By the definitions of  $C_1$  and  $C_2$ , we infer  $\lim_{h \uparrow 1} m(h) = 0 = \lim_{h \uparrow 1} \varphi(h)$ . The combination of (38a) and (39a) recovers (35). Differentiations of the integral equations entail  $m(m^3)_{hh} = -\varphi$ ,  $m\varphi_{hh} = -1$ , by which  $m(m(m^3)_{hh})_{hh} = 1$ .  $\square$

**Corollary 2.** *The constants  $C_1, C_2$  in (35) are positive. Further, for  $0 < h < 1$ , the flux  $\varphi(h)$  is positive; thus, (a twice continuously differentiable)  $m(h)^3$  is concave.*

The first statement in Corollary 2 follows from the definitions of  $C_1, C_2$  and the *assumed* positivity of slope. Note that

$$C_1 = \int_0^1 \frac{1-z}{m(z)} \left[ \int_0^z \frac{\zeta(1-z)}{m(\zeta)} d\zeta + \int_z^1 \frac{z(1-\zeta)}{m(\zeta)} d\zeta \right] dz.$$

The positivity of  $\varphi(h) = -m(m^3)_{hh}$  follows from (39).  $\square$

*Near-facet expansion.* We notice that if  $m(h) = \mathcal{O}(h^\alpha)$  as  $h \downarrow 0$  for some  $0 \leq \alpha < 1$ , the integral terms in (35) generate subdominant contributions of orders (from left to right)  $\mathcal{O}(h^{3-\alpha})$  and  $\mathcal{O}(h^{4-2\alpha})$ . This observation motivates an iteration scheme for (35), or the system of (38a) and (39a). Successive local approximations of  $m(h)$  as  $h \downarrow 0$  can be constructed via the scheme

$$\begin{aligned} m^{(n+1)}(h)^3 &= C_1 h - \int_0^h (h-z) \frac{\varphi^{(n)}(z)}{m^{(n)}(z)} dz, & m^{(0)}(h) &= (C_1 h)^{1/3}; \\ \varphi^{(n+1)}(h) &= C_2 h - \int_0^h \frac{h-z}{m^{(n)}(z)} dz, & \varphi^{(0)}(h) &= C_2 h, \end{aligned} \quad (40)$$

where  $m \sim m^{(n)}$ ,  $\varphi \sim \varphi^{(n)}$  to  $n+1$  terms;  $n = 0, 1, \dots$ . The above construction produces a formal expansion of  $m(h)$  in ascending powers of  $h$ . The first three terms are evaluated in Appendix B.2; the result reads

$$m(h) = (C_1 h)^{1/3} - \frac{3}{40} \frac{C_2}{C_1} h^2 + \frac{27}{700} C_1^{-4/3} h^{8/3} + \mathcal{O}(h^{11/3}) \quad h \downarrow 0. \quad (41)$$

Note the powers of  $h$  entering (41), i.e.,  $1/3$  (leading order),  $2$  (first correction) and  $8/3$ , in comparison to the powers  $1/3, 1, 5/3$  appearing in (30).

In the present setting of self-similarity, we have  $h = h(\eta)$  and  $m(h(\eta)) = h'(\eta)$  where  $\eta = xt^{-1/5}$  [11]. By integration and inversion of (41), we find an expansion of  $m(h(\eta))$  in the vicinity of the facet edge, as  $\bar{\eta} = \eta - \eta_{f,1} \downarrow 0$ :

$$m(h(\eta)) = \left(\frac{2}{3}\right)^{1/2} C_1^{1/2} \bar{\eta}^{1/2} - \frac{8}{315} C_2 \bar{\eta}^3 + \frac{8}{945} \bar{\eta}^4 + \mathcal{O}(\bar{\eta}^{11/2}). \quad (42)$$

Note the absence of the powers  $1, 3/2, 2, 5/2$ ; cf. equation (A5) in [11]. Likewise, by symmetry we can write an expansion for  $m(h)$  as  $h \uparrow 1$ . The above procedure suggests expanding the slope in integer powers of  $\bar{\eta}^{1/2}$  [11].

**Remark 4.** Integral equation (35) can result from integrating the slope ODE  $m[m(m^3)_{hh}]_{hh} = 1$  under the conditions  $m \rightarrow 0$  and  $\varphi \rightarrow 0$  as  $h \downarrow 0$  and  $h \uparrow 1$ . Our technique exemplifies the passage to the continuum limit *via the integral equation* so that these conditions emerge directly from the difference scheme.

**Remark 5.** It is tempting to extend the results of Proposition 2 to the time-dependent setting (without self-similarity), where  $m_j(t) \rightarrow m(h, t)$ . The emergent pair of integral relations for  $m(h, t)$  and the continuum flux,  $\varphi(h, t)$ , is

$$\begin{aligned} m(h, t)^3 &= C_1(t)h - \int_0^h (h-z) \frac{\varphi(z, t)}{m(z, t)} dz, \\ \varphi(h, t) &= C_2(t)h - \int_0^h (h-z) \partial_t [m(z, t)^{-1}] dz, \quad 0 < h < 1, \quad t > 0, \end{aligned} \quad (43)$$

provided the integrals converge;  $C_1(t), C_2(t)$  are subject to the vanishing of  $m$  and  $\varphi$  as  $h \uparrow 1$ . In principle, it may not be legitimate to iterate (43) as above (under self-similarity) in order to obtain an expansion for  $m(h, t)$  near a facet edge, unless  $t$  is sufficiently large. By differentiation of (43), we obtain the familiar PDE  $\partial_t m = -m^2 \partial_h^2 (m \partial_h^2 m^3)$  [11, 22].

**Remark 6.** By (43), the slope is  $m(h(x, t), t) = \mathcal{O}((x - x_f(t))^{1/2})$  as  $x \rightarrow x_f(t)$  (position of a facet edge) for sufficiently long times, consistent with the hypothesis of local equilibrium invoked in earlier continuum theories, e.g., in [22]. Further iterations are suggestive of the nature of the expansion for  $m(h, t)$  in the vicinity of large facet edges. To compute coefficients of the expansion, it is algebraically convenient to make the substitution  $m(h, t) =$

$\sum_{n=1}^{\infty} A_n(t)(x - x_f(t))^{n/2}$  into the PDE for  $m(h, t)$ ; then, the values  $A_2 = A_3 = A_4 = A_5 = 0$  are recovered by dominant balance [11].

### 3.2.2 ADL kinetics

Next, we focus on fourth-order scheme (13), which is also the subject of [1]. By the similarity solution  $m_j(t) = (4t + K)^{-1/4} M_j$ , proved in [1], and  $\psi_j = M_j^3$ , the related difference equations read

$$\psi_{j+2} - 4\psi_{j+1} + 6\psi_j - 4\psi_{j-1} + \psi_{j-2} = f_j = \epsilon^4 \psi_j^{-1/3}, \quad (44a)$$

for  $j = 0, 1, \dots, N - 1$ , along with the conditions

$$\psi_{-1} = 0 = \psi_N, \quad \psi_0 - 2\psi_{-1} + \psi_{-2} = 0 = \psi_{N-1} - 2\psi_N + \psi_{N+1}; \quad (44b)$$

recall that  $\varphi_j = -(\psi_{j+1} - 2\psi_j + \psi_{j-1})$  is the  $j$ th-terrace adatom flux. There are at least two routes to studying (44): either split it into two second-order schemes by using  $\varphi_j$  as an auxiliary variable, or leave the fourth-order scheme intact and use only  $\psi_j$ . We choose the latter way here.

**Proposition 3.** (A continuum limit in ADL kinetics) *In the limit  $\epsilon \downarrow 0$ , discrete scheme (44) reduces to the integral equation*

$$\psi(h) = m(h)^3 = C_1 h - C_3 h^3 + \frac{1}{6} \int_0^h \frac{(h-z)^3}{m(z)} dz, \quad 0 < h < 1; \quad (45)$$

thus,  $\lim_{h \downarrow 0} m(h) = 0 = \lim_{h \downarrow 0} \varphi(h)$  ( $\varphi$ : flux). The constants  $C_1, C_3$  are subject to respective conditions at  $h = 1$ :  $\lim_{h \uparrow 1} m(h) = 0 = \lim_{h \uparrow 1} \varphi(h)$ . By (45), (a sufficiently differentiable)  $m(h)$  satisfies  $m(m^3)_{hhhh} = 1$ ; cf. [1].

By our usual practice, we assume that the integral in (45) converges and a solution exists in some appropriate sense.

**Proof.** We treat the  $f_j$  in (44) as a given forcing term and solve for  $\psi_j$  using (21) and (22), with recourse to a generating polynomial  $\Psi(s)$ ; see Appendix A.2 for details. After some algebra, the variables  $\psi_j$  are found to be

$$\psi_j = \frac{1}{6} \left[ (\psi_1 - 2\psi_0)j^2(j+3) + 2(\psi_0 + \psi_1)j + 6\psi_0 + \epsilon^4 \sum_{p=0}^{j-2} (j-p-1)(j-p)(j-p+1)\psi_p^{-1/3} \right], \quad j = 0, \dots, N-1, \quad (46)$$

where

$$\psi_1 - 2\psi_0 = \frac{-NF(1) + F'(1)}{N+1}, \quad (47a)$$

$$2(N+1)(\psi_1 + \psi_0) = N(2N-1)F(1) + (2N^2 - 5N + 2)F'(1) - 3(N-1)F''(1) + F'''(1), \quad (47b)$$

$$\psi_0 = \frac{N(2N+1)F(1) + N(2N-5)F'(1) - 3(N-1)F''(1) + F'''(1)}{6(N+1)}. \quad (47c)$$

Recall  $F(s) = \sum_{j=0}^{N-1} f_j s^j$ . The prime in (47) denotes the derivative in  $s$ .

Now let  $N \rightarrow \infty$ , and  $\epsilon \downarrow 0$  with  $(N+1)\epsilon = 1$ . By formulas (47), we find

$$\frac{\psi_1 - 2\psi_0}{\epsilon^3} \xrightarrow{\epsilon \downarrow 0} - \int_0^1 \frac{1-z}{m(z)} dz, \quad (48a)$$

$$\frac{\psi_0 + \psi_1}{\epsilon} \xrightarrow{\epsilon \downarrow 0} \frac{1}{2} \int_0^1 \frac{1-z - (1-z)^3}{m(z)} dz, \quad (48b)$$

$$\psi_0 = \mathcal{O}(\epsilon) \rightarrow 0. \quad (48c)$$

For fixed height  $h = (j+1)\epsilon$  (with  $j \rightarrow \infty$ ), we let  $\psi_j \rightarrow \psi(h)$ , thus reducing sum equation (46) to integral equation (45) with

$$C_1 := \lim_{\epsilon \downarrow 0} \frac{\psi_0 + \psi_1}{3\epsilon} = \frac{1}{6} \int_0^1 \frac{1-z - (1-z)^3}{m(z)} dz, \quad (49a)$$

$$C_3 := - \lim_{\epsilon \downarrow 0} \frac{\psi_1 - 2\psi_0}{6\epsilon^3} = \frac{1}{6} \int_0^1 \frac{1-z}{m(z)} dz, \quad (49b)$$

and neglect of  $\psi_0$ . The resulting continuum-scale slope  $m(h)$  vanishes as  $h \downarrow 0$ . In addition,  $\varphi_j \rightarrow \varphi(h)$  with  $\lim_{h \downarrow 0} \varphi(h) = 0$ , as verified directly by (45). Equations (49) imply that the slope and flux also vanish at the other end point, as  $h \uparrow 1$ . The differentiation of (45) furnishes the ODE  $m(m^3)_{hhhh} = 1$  where  $\varphi(h) = -(m^3)_{hh}$ .  $\square$

**Corollary 3.** *The constants  $C_1, C_3$  entering (45) are positive. Further, the large-scale flux,  $\varphi(h) = -(m^3)_{hh}$ , is positive for  $0 < h < 1$ .*

Corollary 3 declares the concavity of  $\psi(h) = m(h)^3$  proved by AKW [1].

In the spirit of Sections 3.1 and 3.2.1, a formal expansion for the slope near facet edges can plausibly be derived by iterations of (45). The ensuing slope behavior is  $m(h) = (C_1 h)^{1/3} + \mathcal{O}(h^{7/3})$  as  $h \downarrow 0$ ; so, the leading-order term is compatible with local equilibrium. Hence, with  $\eta = xt^{-1/4}$ , we have (cf. (42))

$$m(h(\eta)) = \left(\frac{2}{3}\right)^{1/2} C_1^{1/2} \bar{\eta}^{1/2} + \mathcal{O}(\bar{\eta}^{7/2}) \quad \text{as } \bar{\eta} \rightarrow 0; \quad \bar{\eta} = t^{-1/4}(x - x_f(t)). \quad (50)$$

Further details of these computations are left to the interested reader.

**Remark 7.** The derivation can be extended to the full time dependent setting, where  $m_j(t) \rightarrow m(h, t)$ . The integral relation consistent with step laws is

$$m(h, t)^3 = C_1(t)h - C_3(t)h^3 + \frac{1}{6} \int_0^h (h - z)^3 \partial_t [m(z, t)^{-1}] dz , \quad (51)$$

where  $0 < h < 1$  and  $t > 0$ . The PDE reads  $\partial_t m = -m^2 \partial_h^4 m^3$  [1].

## 4 Extensions

In this section we discuss two possible extensions of our formulation. First, we address different laws of nearest-neighbor step interactions; in this case, the slope behavior, i.e., the exponent 1/2 (see Remarks 3 and 6), at facet edges is modified accordingly. Second, we propose a “*toy model*” where the kinetics of attachment-detachment for extremal steps are different from the kinetics for other steps. Our discussion aims to indicate the role that individual steps may play in the derivation of boundary conditions in the continuum setting.

Another plausible extension concerns the presence of an Ehrlich-Schwoebel barrier, by which the attachment-detachment law for all steps is characterized by different kinetic rates, say  $\kappa_u$  and  $\kappa_d$ , for up- and down-steps [8, 35]. In this case, the effective kinetic rate for the adatom flux is the harmonic average of  $\kappa_u$  and  $\kappa_d$  [24]. Our analysis remains essentially intact, leading to the same form of continuum laws. This case is not discussed any further.

### 4.1 Multipole nearest-neighbor step interactions

In this section, we discuss continuum-scale implications of the step energy [24]

$$E_N(\{x_j\}_{j=0}^N) = \frac{1}{\alpha} \sum_{i=0}^{N-1} \left( \frac{\epsilon}{x_{i+1} - x_i} \right)^\alpha = \frac{1}{\alpha} \sum_{i=0}^{N-1} m_i^\alpha \quad \alpha > 1 , \quad (52)$$

which in principle includes step multipole interactions for integer  $\alpha \geq 2$  [27];  $\alpha = 2$  for dipole step interactions. The  $j$ th-step chemical potential is

$$\mu_j = \frac{\delta E_N}{\delta x_j} = \epsilon^{-1} (m_j^{\alpha+1} - m_{j-1}^{\alpha+1}) , \quad j = 1, \dots, N-1 ; \quad (53)$$

in addition,  $\mu_0 = \epsilon^{-1} m_0^{\alpha+1}$  and  $\mu_N = -\epsilon^{-1} m_{N-1}^{\alpha+1}$ . Formulas for the adatom flux and step velocity ensue from Section 2 via  $m_j^3 \mapsto m_j^{\alpha+1}$  in  $\mu_j$ .

For instance, in DL kinetics the discrete scheme for steps now reads

$$\begin{aligned} \frac{\dot{m}_j}{m_j^2} = & -\epsilon^{-4} [m_{j+1}(m_{j+2}^{\alpha+1} - 2m_{j+1}^{\alpha+1} + m_j^{\alpha+1}) - 2m_j(m_{j+1}^{\alpha+1} - 2m_j^{\alpha+1} + m_{j-1}^{\alpha+1}) \\ & + m_{j-1}(m_j^{\alpha+1} - 2m_{j-1}^{\alpha+1} + m_{j-2}^{\alpha+1})], \quad j = 0, \dots, N-1; \end{aligned} \quad (54a)$$

$$m_{-1} = 0 = m_N, \quad m_{-2}, m_{N+1} : \text{finite}. \quad (54b)$$

Thus, the discrete self-similar slopes read  $m_j(t) = [(\alpha + 3)t + K]^{-\frac{1}{\alpha+3}} M_j$ .

To proceed along the lines of Section 3, let  $\psi_j = M_j^{\alpha+1}$ ; or, more generally,  $\psi_j(t) = m_j(t)^{\alpha+1}$ . Our manipulations for  $\psi_j$  remain intact. The analogue of Proposition 2 contains the relation (cf. (35))

$$m(h)^{\alpha+1} = C_1 h - C_2 \int_0^h \frac{z(h-z)}{m(z)} dz + \int_0^h \int_0^z \frac{(h-z)(z-\zeta)}{m(z)m(\zeta)} d\zeta dz, \quad (55)$$

where  $C_1$  and  $C_2$  are subject to the vanishing of slope and flux at  $h = 1$ .

Iterations of (55) yield a formal expansion of the slope near the facet edge ( $h = 0$ ). Accordingly, we obtain  $m(h(x, t), t) = \mathcal{O}((x - x_f(t))^{1/\alpha})$  as  $x \rightarrow x_f(t)$ , the position of a facet edge, for sufficiently long times. This behavior manifests the intimate connection of step interaction law and near-facet expansion at equilibrium [3].

#### 4.2 Special kinetics of extremal step

In this section we explore the following scenario. Suppose the attachment-detachment law for extremal steps ( $j = 0, N$ ) involve kinetic rates, say  $\kappa_L$  for  $j = 0$  and  $\kappa_R$  for  $j = N$ , which may be different from  $\kappa$ . So, according to linear kinetics, the fluxes impinging on these steps are

$$-\varphi_0 = 2\kappa_L(\rho_0 - \rho_0^{\text{eq}}) \quad x = x_0; \quad \varphi_{N-1} = 2\kappa_R(\rho_{N-1} - \rho_N^{\text{eq}}) \quad x = x_N. \quad (56)$$

At the remaining steps, the fluxes have rate  $2\kappa$ . We study whether  $\kappa_L$  or  $\kappa_R$  can possibly distort nontrivially the previous boundary conditions in the macroscopic limit, *assuming this limit is well defined*. Without loss of generality, set  $\kappa_R = \kappa \neq \kappa_L$  and define  $\beta = \kappa_L/\kappa > 0$ ; hence, we restrict attention to the left facet edge ( $h = 0$ ). It is tempting to claim that, in the limit  $\epsilon \downarrow 0$ , the detail of (56) *disappears* and we recover a continuum-scale boundary condition of zero slope and flux. We discuss formally why this claim is consistent with steps if  $\beta = \mathcal{O}(1)$ . The situation is subtler if  $\beta = \mathcal{O}(\epsilon^\gamma)$ ,  $\gamma > 0$ .

The 0-th terrace adatom flux is  $\varphi_0 = -\epsilon^{-1} (\bar{\kappa}\epsilon)m_0 (\rho_1^{\text{eq}} - \rho_0^{\text{eq}})/(\bar{\kappa}\epsilon + m_0)$  where  $\bar{\kappa} = (\kappa^{-1} + \kappa_L^{-1})^{-1}$ . We focus on ADL kinetics, where surface processes are limited by atom attachment-detachment at steps, and scale time by  $\kappa\epsilon$  (as in

Section 2.2). The motion laws for the discrete slopes are described by (13a) along with the *partially modified* termination conditions

$$m_{-1}^3 + (1 - \beta)(m_1^3 - 2m_0^3) = 0 = m_N^3, \quad (57a)$$

$$m_0^3 - 2m_{-1}^3 + m_{-2}^3 = 0 = m_{N-1}^3 - 2m_N^3 + m_{N+1}^3. \quad (57b)$$

Equations (57b) state that the auxiliary discrete fluxes vanish, in accord with (13b); hence, we expect that the boundary conditions for the continuum-scale flux are intact. By contrast, (57a) indicates a nonzero  $m_{-1}$ , which in turn suggests the possibility of a nonzero continuum-scale slope as  $h \downarrow 0$ . (Note, however, that in view of (57a) the mirror symmetry of the system is removed.)

We proceed to convert (13a) to sum equations via generating polynomials from Appendix A.2; let  $\psi_j = m_j^3$ . After some algebra, we find (cf. (46))

$$\begin{aligned} \psi_j = \frac{1}{6} \left\{ \beta(\psi_1 - 2\psi_0)j^2(j+3) + 2[\psi_0 + \psi_1 - 2(\beta-1)(\psi_1 - 2\psi_0)]j + 6\psi_0 \right. \\ \left. + \epsilon^4 \sum_{p=0}^{j-2} (j-p-1)(j-p)(j-p+1)(d/dt)\psi_j(t)^{-1/3} \right\}, \quad (58) \end{aligned}$$

where, with  $F(s) = \epsilon^4 \sum_{j=0}^{N-1} s^j (d/dt)\psi_j(t)^{-1/3}$ , the requisite coefficients are

$$\beta(\psi_1 - 2\psi_0) = \frac{-NF(1) + F'(1)}{N+1},$$

$$\begin{aligned} 2(N+1)[\psi_0 + \psi_1 - 2(\beta-1)(\psi_1 - 2\psi_0)] = \left( 2N^2 - N + 6\frac{\beta-1}{\beta} \frac{N}{N+1} \right) F(1) \\ + \left( 2N^2 - 5N + 2 - 6\frac{\beta-1}{\beta} \frac{1}{N+1} \right) F'(1) - 3(N-1)F''(1) + F'''(1), \end{aligned}$$

$$\begin{aligned} 6(N+1)\psi_0 = \left( 2N^2 + N - 6N\frac{\beta-1}{\beta} \frac{N}{N+1} \right) F(1) + \left( 2N^2 - 5N \right. \\ \left. + 6\frac{\beta-1}{\beta} \frac{N}{N+1} \right) F'(1) - 3(N-1)F''(1) + F'''(1). \end{aligned}$$

Note the term  $\psi_0$  entering the right-hand side of (58). *The question arises as to whether  $\psi_0 = \mathcal{O}(1)$  as  $\epsilon \downarrow 0$  by manipulation of  $\beta$ .*

Consider the limit of (58) as  $N \rightarrow \infty$  with  $\epsilon(N+1) = 1$ . By inspection of the preceding formulas and repetition of the procedure of Section 3.2.2,

we infer that any contribution of  $\beta$  is negligible if  $\beta = \mathcal{O}(1)$ . In this case, the macroscopic laws are identical to those for  $\beta = 1$  (Section 3.2.2); so, the slope *and* flux vanish at the facet edges. These conditions appear to persist provided  $\beta > \mathcal{O}(N^{-3})$ . In particular, the flux vanishes at  $h = 0, 1$  for any  $\beta > 0$  (provided the continuum limit is meaningful). A possibility for nonzero slope as  $h \downarrow 0$  may arise if  $\beta = \mathcal{O}(N^{-3})$ .

Entertaining the scenario of a small, extreme  $\beta$ , suppose  $\beta = \check{\beta}/N^3$ ,  $\check{\beta} = \mathcal{O}(1) > 0$ , while the macroscopic limit makes sense, e.g.,  $N^{4-n}F^{(n)}(1) \rightarrow \int_0^1 z^{n-1} \partial_t [m(z, t)^{-1}] dz = \mathcal{O}(1)$  as  $N \rightarrow \infty$ ;  $n = 1, 2, 3, 4$  and  $F^{(n)}(s)$  denotes the  $n$ th-order derivative of  $F(s)$ . By dominant balance we wind up with

$$m(h, t)^3 = C_0(t) + C_1(t)h - C_3(t)h^3 + \frac{1}{6} \int_0^h (h - z)^3 \partial_t [m(z, t)^{-1}] dz ; \quad (59)$$

cf. (51). The coefficients  $C_0(t)$ ,  $C_1(t)$ ,  $C_3(t)$  are found to be

$$C_0(t) = \lim_{\epsilon \downarrow 0} \psi_0(t) = \check{\beta}^{-1} \int_0^1 (1 - z) \partial_t [m(z, t)^{-1}] dz ,$$

which signifies the nonzero value of the continuum slope as  $h \downarrow 0$ , and

$$\begin{aligned} C_1(t) &= \lim_{\epsilon \downarrow 0} \frac{\psi_1(t) + \psi_0(t) - 2(\beta - 1)[\psi_1(t) - 2\psi_0(t)]}{3\epsilon} \\ &= \frac{1}{6} \int_0^1 [(1 - 6\check{\beta}^{-1})(1 - z) - (1 - z)^3] \partial_t [m(z, t)^{-1}] dz , \end{aligned}$$

$$C_3(t) = - \lim_{\epsilon \downarrow 0} \frac{\beta[\psi_1(t) - 2\psi_0(t)]}{6\epsilon^3} = \frac{1}{6} \int_0^1 (1 - z) \partial_t [m(z, t)^{-1}] dz .$$

Note that if  $\check{\beta} \gg 1$ , (59) reduces to the macroscopic limit of Section 3.2.2.

A sufficiently small  $\beta$  forces the microscale flux at the top step to become small; thus, the motion of the extremal step tends to be frozen and the density of steps increases in the vicinity of the left facet edge. Interestingly, our heuristic analysis indicates the critical scaling  $\mathcal{O}(N^{-3})$  for  $\beta$ .

## 5 Conclusion and discussion

Inspired by a recent analysis of ADL kinetics for a finite crystal [1], we derived formal expansions for the continuum surface slope in the vicinity of semi-infinite crystal facets located at fixed heights. Our starting point was a system of nonlinear ODEs for discrete slopes in 1D according to the BCF model. Each of the steps interacts with its nearest neighbors through elastic-dipole and entropic repulsions. The ODEs were converted to a difference scheme and

sum equations via a discrete self-similar solution. In the macroscopic limit, the sum equations are reduced to integral relations which unveil via iterations the local behavior of the continuum slope (and flux) near facets. Our approach is not limited by the kinetics: evaporation-condensation as well as DL and ADL kinetics in surface diffusion are treated formally on the same grounds.

We studied two possible extensions of this approach. First, we considered multipole nearest-neighbor step interactions. For step interactions decaying as  $w^{-\alpha}$  with the terrace width  $w$ , where  $\alpha \geq 2$ , the slope vanishes as  $\mathcal{O}(\bar{x}^{1/\alpha})$  with the distance  $\bar{x}$  from the facet edge, in agreement with notions of local equilibrium. Second, we studied implications of special kinetics at extremal steps, assuming the macroscopic limit is meaningful.

Our setting, motivated by [1, 11], provides an explicit example of a step flow model consistent with the continuum theory. The conditions of zero slope and flux (e.g., in DL kinetics) are compatible with those afforded by a gradient-flow-type formulation; see, e.g., Odisharia [29], Spohn [39], and Shenoy and Freund [36]. Our work provides a linkage of the underlying particle structure to the local behavior of continuum-scale variables near the facet boundary.

Our approach bears limitations. The self-similar solution studied here captures the long-time evolution of the slope; the transient near-facet behavior requires a subtler analysis. The derived integral equations have not been studied rigorously; so, issues of existence and uniqueness of solutions were not touched upon. In the same vein, the legitimacy of applying iterations was not addressed, although an exactly solvable case (in evaporation-condensation via self-similarity) was pointed out. Self-similar solutions were applied but not proved to exist, be unique or stable.

In our setting the facets are semi-infinite, 1D and located at fixed heights. This assumption simplifies (the more realistic) situations where facets are finite, have curved boundaries and time-varying height [15, 23]. In such cases, individual steps collapsing on top of the facets can influence the surface profile macroscopically [15]. The derivation of near-facet expansions for the slope in more complicated geometries is the subject of work in progress.

## Acknowledgments

The first author's (DM) research was supported by NSF DMS0847587 at the University of Maryland. We wish to thank Robert V. Kohn, Hala Al Hajj Shehadeh and Jonathan Weare for bringing preprint [1] to our attention and sharing with us details of their work. The first author also thanks Pak-Wing Fok, Manoussos Grillakis, David Levermore, Rodolfo Ruben Rosales, Howard

Stone, and John Weeks for useful discussions.

## A On solutions of difference equations

In this appendix, we provide details of basic computations needed in Section 3. In particular, we elaborate on the derivation of (25), (36), (37) and (46) and the associated coefficients.

### A.1 Second-order difference scheme

Consider the difference scheme

$$\psi_{j+1} - 2\psi_j + \psi_{j-1} = f_j, \quad j = 0, \dots, N-1; \quad \psi_{-1} = 0 = \psi_N, \quad (\text{A.1})$$

where  $f_j$  can be time dependent but the time is suppressed since it is immaterial here. By multiplying (A.1) by  $s^j$  and summing over  $j$  we have

$$s^{-1}[\Psi(s) - \psi_0 + \psi_N s^N] - 2\Psi(s) + s[\Psi(s) + \psi_{-1}s^{-1} - \psi_{N-1}s^{N-1}] = F(s),$$

where  $F(s)$  is defined in (23). Thus, we obtain

$$\Psi(s) = \frac{\psi_0 - \psi_{-1}s - \psi_N s^N + \psi_{N-1}s^{N+1} + sF(s)}{(1-s)^2} = \frac{\mathcal{P}(s)}{(1-s)^2}, \quad (\text{A.2})$$

which leads to (23) by virtue of the termination conditions. The point  $s = 1$  is a removable singularity provided  $\mathcal{P}(1) = 0 = \mathcal{P}'(1)$ , which yield (24).

The coefficient of  $s^j$  in  $\Psi(s)$  is given by (21). By restricting the contour  $\Gamma$  in the interior of the unit disk ( $|\zeta| < 1$ ) and eliminating analytic terms, we have

$$\psi_j = \frac{1}{2\pi i} \oint_{\Gamma} \frac{\psi_0 + \zeta F(\zeta)}{(1-\zeta)^2} \frac{d\zeta}{\zeta^{j+1}}, \quad j = 0, \dots, N-1. \quad (\text{A.3})$$

Recalling the binomial expansion  $(1-\zeta)^{-2} = \sum_{k=0}^{\infty} (1+k)\zeta^k$ , we find the series

$$\frac{\psi_0 + \zeta F(\zeta)}{(1-\zeta)^2} = \psi_0 + \sum_{l=0}^{\infty} \zeta^{l+1} \left[ l+2 + \sum_{p=0}^l (1+l-p)f_p \right]. \quad (\text{A.4})$$

The coefficient of  $\zeta^j$  is singled out for  $l = j-1$ ; thus, by (A.3) we recover (25). The derivation of (36) and (37) follows from the same procedure.

## A.2 Fourth-order difference scheme

Next, consider the difference scheme (44). The generating polynomial,  $\Psi(s)$ , introduced in (22) satisfies

$$\begin{aligned} & s^{-2}(\Psi - \psi_0 - \psi_1 s + \psi_N s^N + \psi_{N+1} s^{N+1}) - 4s^{-1}(\Psi - \psi_0 + \psi_N s^N) \\ & + 6\Psi - 4s(\Psi + \psi_{-1} s^{-1} - \psi_{N-1} s^{N-1}) + s^2(\Psi + \psi_{-2} s^{-2} + \psi_{-1} s^{-1} \\ & - \psi_{N-1} s^{N-1} - \psi_{N-2} s^{N-2}) = F(s) = \sum_{j=0}^{N-1} f_j s^j . \end{aligned}$$

In view of termination conditions (44b), we thus find

$$\Psi(s) = \frac{\mathcal{P}(s)}{(1-s)^4} , \quad (\text{A.5a})$$

where the numerator is

$$\begin{aligned} \mathcal{P}(s) = & \psi_0 + (\psi_1 - 4\psi_0)s + \psi_0 s^2 + \psi_{N-1} s^{N+1} + (\psi_{N-2} - 4\psi_{N-1})s^{N+2} \\ & + \psi_{N-1} s^{N+3} + s^2 F(s) . \end{aligned} \quad (\text{A.5b})$$

Clearly, the point  $s = 1$  must be a removable singularity in (A.5a); thus, we should have  $\mathcal{P}(1) = \mathcal{P}'(1) = \mathcal{P}''(1) = \mathcal{P}'''(1) = 0$ , which entail a system of equations for the parameters  $\psi_0, \psi_1, \psi_{N-2}, \psi_{N-1}$ :

$$\begin{aligned} & \psi_1 - 2\psi_0 + \psi_{N-2} - 2\psi_{N-1} = -F(1) , \\ & \psi_1 - 2\psi_0 + (N+2)(\psi_{N-2} - 2\psi_{N-1}) = -2F(1) - F'(1) , \\ & 2\psi_0 + (N+1)(N+2)\psi_{N-2} - 2(N^2 + 3N + 1)\psi_{N-1} = -2F(1) \\ & \quad - 4F'(1) - F''(1) , \\ & N(N+1)(N+2)\psi_{N-2} - 2(N^2 - 1)(N+3)\psi_{N-1} = -6[F'(1) \\ & \quad + F''(1)] - F'''(1) . \end{aligned} \quad (\text{A.6})$$

The solution of this system leads to formulas (47).

Next, we determine  $\psi_j$  in terms of  $\psi_0, \psi_1$  with recourse to (21);  $\Gamma$  is a contour enclosing 0 in the interior of the unit disk. By removing the analytic part of the integrand, we have (for  $j = 0, \dots, N-1$ )

$$\psi_j = \frac{1}{2\pi i} \oint_{\Gamma} \frac{\psi_0 + (\psi_1 - 4\psi_0)\zeta + \psi_0 \zeta^2 + \zeta^2 F(\zeta)}{(1-\zeta)^4} \frac{d\zeta}{\zeta^{j+1}} . \quad (\text{A.7})$$

By virtue of the binomial expansion

$$(1 - \zeta)^{-4} = \frac{1}{3!} \sum_{l=0}^{\infty} (l+1)(l+2)(l+3)\zeta^l \quad |\zeta| < 1 ,$$

the integrand in (A.7) has residue equal to

$$\frac{1}{3!} \left[ \psi_0(j+1)(j+2)(j+3) + (\psi_1 - 4\psi_0)j(j+1)(j+2) + \psi_0(j-1)j(j+1) + \sum_{p=0}^{j-2} (j-1-p)(j-p)(j-p+1)f_p \right] .$$

By separating distinct powers of  $j$  in the first line, we obtain (46).

## B Iterations of integral equations

In this appendix, we discuss the integral equations of Section 3, especially the use of iterations for formally constructing expansions of solutions near facet edges. The case with evaporation-condensation serves as a paradigm for validation of the iteration procedure, since a simple exact, global similarity solution for the slope is derived independently.

### B.1 Evaporation-condensation

*Iteration scheme.* Consider the sequence  $\{m^{(n)}(h)\}_{n=0}^{\infty}$  defined by (29). On the basis of the proposed scheme, we compute

$$\begin{aligned} n = 1 : \quad m^{(1)}(h) &= \left( C_1 h - \frac{9}{10} C_1^{-1/3} h^{5/3} \right)^{1/3} \\ \Rightarrow m^{(1)}(h) - m^{(0)}(h) &= -\frac{3}{10} C_1^{-1} h + \mathcal{O}(h^{5/3}) \quad \text{as } h \downarrow 0 . \end{aligned} \quad (\text{B.1})$$

More generally, the difference  $\delta m^{(n)} = m^{(n)} - m^{(n-1)}$  satisfies

$$\delta m^{(n)} [m^{(n)2} + m^{(n)} m^{(n-1)} + m^{(n-1)2}] (h) = \int_0^h \frac{(h-z) \delta m^{(n-1)}(z)}{m^{(n-1)}(z) m^{(n-2)}(z)} dz \quad (\text{B.2})$$

for  $n = 2, \dots$ ;  $m^{(n)}(h) \sim (C_1 h)^{1/3}$  for every  $n$  as  $h \downarrow 0$ . By inspection of (B.1) and (B.2), we see that  $\delta m^{(n)}(h) \sim a_n h^{b_n}$ . For instance, for  $n = 2$  we compute

$a_2 = -(9/280)C_1^{-7/3}$ ,  $b_2 = 5/3$  and

$$m^{(2)} \sim m^{(1)}(h) - \frac{9}{280}C_1^{-7/3}h^{5/3} = \left(C_1h - \frac{9}{10}C_1^{-1/3}h^{5/3}\right)^{1/3} - \frac{9}{280}C_1^{-7/3}h^{5/3} ,$$

which immediately leads to the three-term expansion (30) for  $m(h)$ . Higher-order terms are generated in an analogous fashion, but of course the algebra becomes increasingly cumbersome with the order,  $n$ .

*Global similarity solution.* It is rather fortuitous that  $m(h)$  can be determined globally [12], thus rendering possible a comparison with expansion (30). By  $\psi(h) = m(h)^3$ , the governing ODE is  $\psi'' = -\psi^{-1/3}$ , where the prime denotes the derivative in  $h$ . If  $\psi(0) = 0 = \psi(1)$ , by symmetry we can restrict  $\psi(h)$  in  $(0, 1/2)$  where  $\psi'(h) \geq 0$  and  $\psi'(1/2) = 0$ . The ODE is split into the system

$$\psi' = w , \quad w' = -\psi^{-1/3} , \quad (\text{B.3})$$

to which we associate a constant of motion via the ‘‘energy’’

$$\mathcal{E}(h) = \frac{1}{2}w(h)^2 + \frac{3}{2}\psi(h)^{2/3}; \quad \mathcal{E}'(h) = 0 . \quad (\text{B.4})$$

Thus, solutions of (B.3) can be parametrized by the constant  $c = \mathcal{E}(h)$ .

Suppose that we look for solutions consistent with integral equation (19). So, we require that  $\psi$ ,  $w$  solve (B.3) for  $h \in (0, 1/2)$  under the conditions

$$\psi(0) = 0 , \quad w(1/2) = 0 . \quad (\text{B.5})$$

By definition of  $\mathcal{E}$  and  $w$  we compute  $h(m)$  by

$$h = \int_0^\psi \frac{d\xi}{\sqrt{2c - 3\xi^{2/3}}} = \frac{c}{\sqrt{3}} \left( \sin^{-1} \tilde{m} - \tilde{m} \sqrt{1 - \tilde{m}^2} \right); \quad \tilde{m} = m \sqrt{\frac{3}{2c}} \quad (\text{B.6})$$

and  $0 \leq h \leq 1/2$  along with  $w = d\psi/dh \geq 0$ . The solution  $h(m)$  for  $1/2 < h \leq 1$  is obtained by reflection. In principle, (B.6) (and its reflection) can be inverted to generate  $m(h)$ . The constant  $c$  can be found by setting  $h = 1/2$  in (B.6) and using the definition of  $\mathcal{E}(h)$  and  $w(1/2) = 0$ . Thus, we deduce

$$\frac{1}{2} = \int_0^{\psi(1/2)} \frac{d\xi}{\sqrt{2c - 3\xi^{2/3}}} , \quad c = 3\psi(1/2)^{2/3}/2 \Rightarrow c = \sqrt{3}/\pi , \quad (\text{B.7})$$

and  $m(1/2) = 3^{-1/4}2^{1/2}\pi^{-1/2}$ .

We proceed to generate a power series of  $m(h)$  in  $h$  by inversion of (B.6). We write the Maclaurin expansion

$$\pi h = \sum_{l=1}^{\infty} \frac{\Gamma(\frac{1}{2} + l)}{l! \Gamma(\frac{1}{2})} \frac{4l}{4l^2 - 1} \tilde{m}^{2l+1} \quad \tilde{m} < 1 ,$$

where  $\Gamma(z)$  is the usual Gamma function. The inversion of the last series up to three terms yields

$$\widetilde{m}(h)^3 = \frac{3\pi h}{2} - \frac{3}{10} \left( \frac{3\pi h}{2} \right)^{5/3} - \frac{3}{280} \left( \frac{3\pi h}{2} \right)^{7/3} + \mathcal{O}(h^3) \quad \text{as } h \downarrow 0. \quad (\text{B.8})$$

This expansion is in agreement with (30) provided  $C_1 = 3^{1/4} 2^{1/2} \pi^{-1/2}$ . It is worthwhile noting that the complete  $h$ -expansion produced by inversion of the exact solution is convergent in a neighborhood of  $h = 0$ .

## B.2 DL kinetics

Consider scheme (40). Because of the increasingly elaborate algebra, we compute up to three terms for  $m(h(\eta))$ .

$$m^{(1)}(h)^3 = C_1 h - \int_0^h \frac{h-z}{(C_1 z)^{1/3}} C_2 z \, dz = C_1 h - \frac{9}{40} \frac{C_2}{C_1^{1/3}} h^{8/3}, \quad (\text{B.9})$$

$$\varphi^{(1)}(h) = C_2 h - \int_0^h \frac{h-z}{(C_1 z)^{1/3}} \, dz = C_2 h - \frac{9}{10} C_1^{-1/3} h^{5/3};$$

$$\Rightarrow \frac{\varphi^{(1)}(h)}{m^{(1)}(h)} = \frac{C_2}{C_1^{1/3}} h^{2/3} - \frac{9}{10} C_1^{-2/3} h^{4/3} + \mathcal{O}(h^{7/3}) \quad h \downarrow 0.$$

Accordingly, an approximation for  $m^{(2)}(h)$  comes from

$$\begin{aligned} m^{(2)}(h)^3 &= C_1 h - \int_0^h (h-z) \frac{\varphi^{(1)}(z)}{m^{(1)}(z)} \\ &= C_1 h - \frac{9}{40} \frac{C_2}{C_1^{1/3}} h^{8/3} + \frac{3^4}{700} C_1^{-2/3} h^{10/3} + \mathcal{O}(h^{13/3}), \end{aligned} \quad (\text{B.10})$$

which leads to (41) where  $m(h(\eta)) = h'(\eta)$ . By integrating in  $\eta$  we find

$$\bar{\eta} = \frac{3}{2} C_1^{-1/3} h^{2/3} + \frac{9}{280} \frac{C_2}{C_1^{5/3}} h^{7/3} - \frac{9}{700} C_1^{-2} h^3 + \mathcal{O}(h^4) \quad h \downarrow 0.$$

The inversion of this expansion yields

$$h(\eta) = \left( \frac{2}{3} \right)^{3/2} C_1^{1/2} \bar{\eta}^{3/2} - \frac{2}{315} C_2 \bar{\eta}^4 + \frac{8}{4725} \bar{\eta}^5 + \mathcal{O}(\bar{\eta}^{13/2}), \quad (\text{B.11})$$

which is reduced to (42) through differentiation.

## References

- [1] H. Al Hajj Shehadeh, R. V. Kohn, J. Weare, The evolution for a 1-dimensional crystal of finite size: the ADL case, preprint.
- [2] A. Bonito, R. H. Nochetto, J. Quah, D. Margetis, Self-organization of decaying surface corrugations: A numerical study, *Phys. Rev. E* 79 (2009) 050601.
- [3] H. P. Bonzel, 3D equilibrium crystal shapes in the new light of STM and AFM, *Phys. Rep.* 385 (2003) 1–67.
- [4] W. K. Burton, N. Cabrera, F. C. Frank, The growth of crystals and the equilibrium structure of their surfaces, *Philos. Trans. R. Soc. London Ser. A* 243 (1951) 299–358.
- [5] G. F. Carrier, M. Krook, C. E. Pearson, *Functions of a Complex Variable: Theory and Technique*, McGraw-Hill, New York, 1966.
- [6] A. Chame, S. Rousset, H. P. Bonzel, J. Villain, Slow dynamics of stepped surfaces, *Bulgarian Chem. Commun.* 29 (1996/97) 398–434.
- [7] W. E, N. K. Yip, Continuum theory of epitaxial growth. I, *J. Stat. Phys.* 104 (2001) 221–253.
- [8] G. Ehrlich, F. Hudda, Atomic view of surface diffusion: Tungsten on tungsten, *J. Chem. Phys.* 44 (1966) 1039–1099.
- [9] J. W. Evans, P. A. Thiel, M. C. Bartelt, Morphological evolution during epitaxial thin film growth: Formation of 2D islands and 3D mounds, *Surf. Sci. Rep.* 61 (2006) 1–128.
- [10] P.-W. Fok, R. R. Rosales, D. Margetis, Unification of step bunching phenomena on vicinal surfaces, *Phys. Rev. B* 76 (2007) 033408.
- [11] P.-W. Fok, R. R. Rosales, D. Margetis, Facet evolution on supported nanostructures: the effect of finite height, *Phys. Rev. B* 78 (2008) 235401.
- [12] M. G. Grillakis, private communication, 2010.
- [13] E. E. Gruber, W. W. Mullins, On the theory of anisotropy of crystalline surface tension, *J. Phys. Chem. Solids* 28 (1967) 875–887.
- [14] D. T. J. Hurle (Ed.), *Handbook of Crystal Growth*, North Holland, Amsterdam, 1993.
- [15] N. Israeli, D. Kandel, Profile of a decaying crystalline cone, *Phys. Rev. B* 60 (1999) 5946–5962.
- [16] N. Israeli, D. Kandel, Decay of one-dimensional surface modulations, *Phys. Rev. B* 62 (2000) 13707–13717.
- [17] N. Israeli, H.-C. Jeong, D. Kandel, J. D. Weeks, Dynamics and scaling of one-dimensional surface structures, *Phys. Rev. B* 61 (2000) 5698–5706.

- [18] C. Jayaprakash, W. F. Saam, S. Teitel, Roughening and facet formation in crystals, *Phys. Rev. Lett.* 50 (1983) 2017–2020.
- [19] H.-C. Jeong, E. D. Williams, Steps on surfaces: experiments and theory, *Surf. Sci. Rep.* 34 (1999) 171–294.
- [20] R. V. Kohn, T. S. Lo, N. K. Yip, Continuum limit of a step flow model of epitaxial growth, in: M. C. Bartelt, J. W. Evans, A. S. Karma, S. Torquato, D. E. Wolf (Eds.), *Statistical Mechanical Modeling in Materials Science*, MRS Symposia Proceedings No. 701, Materials Research Society, Warrendale, PA, 2002, pp. T1.7.1–T1.7.7.
- [21] V. I. Marchenko, A. Ya. Parshin, Elastic properties of crystal surfaces, *Sov. Phys. JETP* 52 (1980) 129–131.
- [22] D. Margetis, M. J. Aziz, H. A. Stone, Continuum approach to self-similarity and scaling in morphological relaxation of a crystal with a facet, *Phys. Rev. B* 71 (2005) 165432.
- [23] D. Margetis, P.-W. Fok, M. J. Aziz, H. A. Stone, Continuum theory of nanostructure decay via a microscale condition, *Phys. Rev. Lett.* 97 (2006) 096102.
- [24] D. Margetis, R. V. Kohn, Continuum relaxation of interacting steps on crystal surfaces in 2+1 dimensions, *Multisc. Model. Simul.* 5 (2006) 729–758.
- [25] D. Margetis, A. E. Tzavaras, Kinetic hierarchies and macroscopic limits for crystalline steps in 1+1 dimensions, *Multisc. Model. Simul.* 7 (2009) 1428–1454.
- [26] T. Michely, J. Krug, *Islands, Mounds and Atoms: Patterns and Processes in Crystal Growth Far From Equilibrium*, Springer, Berlin, 2004.
- [27] R. Najafabadi, J. R. Srolovitz, Elastic step interactions on vicinal surfaces of fcc metals, *Surf. Sci.* 317 (1994) 221–234.
- [28] P. Nozières, On the motion of steps on a vicinal surface, *J. Phys. (France)* 48 (1987) 1605–1608.
- [29] I. V. Odisharia, *Simulation and analysis of the relaxation of a crystalline surface*, Ph.D. Thesis, New York University, 2006.
- [30] M. Ozdemir, A. Zangwill, Morphological equilibration of a corrugated crystalline surface, *Phys. Rev. B* 42 (1990) 5013–5024.
- [31] O. Pierre-Louis, Dynamics of crystal steps, *C. R. Phys.* 6 (2005) 11–21.
- [32] A. Pimpinelli, J. Villain, *Physics of Crystal Growth*, Cambridge, UK, 1998.
- [33] M. Pulvirenti, Kinetic limits for stochastic particle systems, in: D. Talay and L. Tubaro (Eds.), *Lecture Notes in Mathematics*, Vol. 1627, pp. 96–126, Springer, Berlin, 1996.
- [34] A. Rettori, J. Villain, Flattening of grooves on a crystal surface: A method of investigation of surface roughness, *J. Phys. (France)* 49 (1988) 257–267.

- [35] R. L. Schwoebel, E. J. Shipsey, Step motion on crystal surfaces, *J. Appl. Phys.* 37 (1966) 3682–3686.
- [36] V. B. Shenoy, L. B. Freund, A continuum description of the energetics and evolution of stepped surfaces in strained nanostructures, *J. Mech. Phys. Solids* 50 (2002) 1817–1841.
- [37] V. B. Shenoy, A. Ramasubramaniam, H. Ramanarayan, D. T. Tambe, W.-L. Chan, E. Chason, Influence of step-edge barriers on the morphological relaxation of nanoscale ripples on crystal surfaces, *Phys. Rev. Lett.* 92 (2004) 256101.
- [38] H. Spohn, *Large Scale Dynamics of Interacting Particles*, Springer, Berlin, 1991.
- [39] H. Spohn, Surface dynamics below the roughening transition, *J. Phys. I (France)* 3 (1993) 69–81.
- [40] H. A. Stone, M. J. Aziz, D. Margetis, Grooving of a grain boundary by evaporation-condensation below the roughening transition, *J. Appl. Phys.* 97 (2005) 113535.
- [41] Y. Xiang, Derivation of a continuum model for epitaxial growth with elasticity on vicinal surface, *SIAM J. Appl. Math.* 63 (2002) 241–258.